Magnitude-Phase Optical OFDM for IM/DD Communication Systems

Jie Lian and Maïté Brandt-Pearce
Charles L. Brown Department of Electrical and Computer Engineering
University of Virginia, Charlottesville, VA 22904
Email: jl5qn@virginia.edu, mb-p@virginia.edu

***Abstract*—Orthogonal frequency division multiplexing (OFDM) is a candidate technique to provide high-speed data transmissions for optical communication systems. For intensity modulation and direct detection (IM/DD) optical communication systems, only real and non-negative valued signals can be transmitted due to the natural properties of the transmitters and receivers. This paper proposes a technique called *magnitude-phase optical OFDM* (MPO-OFDM) that transmits the magnitude and phase of the conventional complex valued OFDM signal successively, similar to polar-based OFDM. Unlike polar-based OFDM, however, the proposed MPO-OFDM quantizes, encodes, and transmits the phase information using pulse amplitude modulation (PAM) to reduce the interference introduced by the additive noise on the phase. Considering the peak radiation power constraint of optical devices, the magnitude component of the MPO-OFDM signal experiences clipping distortion. In this paper, we optimally adjust the modulation index to control the scale of the magnitude component and achieve the highest signal to noise ratio (SNR). For the same transmitted data rate, the proposed MPO-OFDM can achieve a lower bit error rate than previously proposed techniques. For a similar BER performance, MPO-OFDM can support a higher throughput than the other techniques tested.**

***Index Terms*—Intensity modulation/direct detection, optical wireless communications, phase noise, quantization, OFDM.**

I. Introduction

Intensity modulation and direct detection (IM/DD) communication systems, such as free space optical communications, visible light communications, and infrared communications, have attracted much research attention recently [1], [2]. Using light emitting diodes (LEDs) or laser diodes (LDs) as transmitters, IM/DD optical systems have many advantages over ratio-frequency (RF) communications, including high privacy, high data rate, low power consumption, and no spectrum regulation. However, the natural properties of LDs, LEDs, and photodetectors (PDs) operated in IM/DD mode require the transmitted and received signals to be non-negative and real-valued. This necessitates special considerations when choosing a modulation scheme.

Recently, orthogonal frequency division multiplexing (OFDM) has been proposed for IM/DD systems due to its high spectral efficiency and resistance to inter-symbol interference (ISI) [3]–[5]. Since non-negative and real-valued signals should be transmitted, conventional OFDM cannot be applied directly in IM/DD systems. Some modified optical OFDM techniques have been proposed to generate appropriate signals for IM/DD systems using Hermitian symmetry. DC-biased optical OFDM (DCO-OFDM) is the most commonly used optical OFDM technique because of its simplicity [6]. To make the bipolar OFDM signal unipolar, a DC-bias (usually half of the peak transmitted power) is added. However, the DC bias requires extra power, and the peak power constraint may introduce more distortion due to the signal offset. Asymmetrically clipped optical OFDM (ACO-OFDM) only modulates the odd frequency subcarriers, which results in a low bandwidth utilization efficiency [7], [8]. Combining ACO-OFDM with pulse position modulation, some researchers proposed a technique called fractional reverse polarity optical OFDM, which takes dimming control into consideration for visible light communications applications [9]. Unipolar OFDM (U-OFDM) (also known as Flip-OFDM) is a recently proposed alternative technique that does not require a DC bias and can generate unipolar signals by sending the positive and negative parts of the bipolar original signal successively in two time slots [10]. However, the required bandwidth for U-OFDM is twice larger than DCO-OFDM when transmitting the same OFDM symbol rate.

To generate real signals, the techniques above use Hermitian symmetry by sacrificing a half of the total subcarriers. A polar-based OFDM has been proposed to generate real and positive-valued signals without using Hermitian symmetry [11]. In [11], the magnitude and phase information of the original OFDM signal are transmitted successively in two adjacent frames. However, the noise added to the phase frame severely impacts the system performance.

In this paper, we propose a modified polar-based OFDM we call magnitude-phase optical OFDM (MPO-OFDM), for IM/DD systems. In this method, Hermitian symmetric data at the input to the OFDM modulator is not required to generate real signals. Instead, the magnitude and phase components of the conventional complex-valued OFDM signals are transmitted successively. Unlike polar-based OFDM, the proposed MPO-OFDM quantizes the phase information and sends it using M-ary pulse amplitude modulation (M-PAM). Using M-PAM, the effects of the noise on the phase component can be reduced. However, because of the peak transmitted power constraint, the magnitude component experiences non-linear distortion, as in polar-based OFDM. The modulation index that controls the scale of the magnitude component is optimized in this paper to maximize the signal to noise ratio (SNR) for the magnitude component. Compared

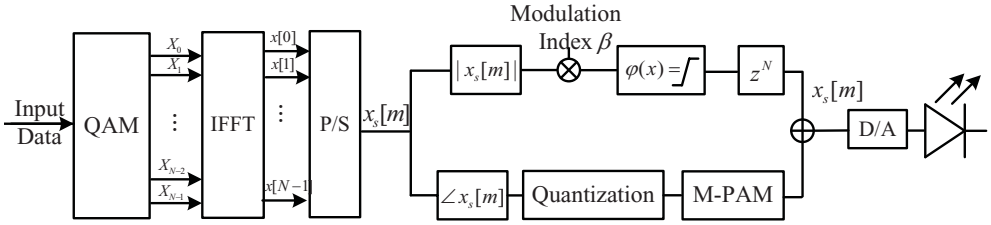

Fig. 1. Block diagram of the transmitter in MPO-OFDM systems.

with DCO-, ACO-, U-OFDM and polar-based OFDM, the proposed MPO-OFDM can provide a better bit error rate (BER) performance.

The remainder of the paper is organized as follows. The principles of MPO-OFDM are described in Section II. Numerical and simulation results are discussed in Section III. Finally, the paper is concluded in Section IV.

II. MPO-OFDM Description

This section describes the principles of MPO-OFDM, and provides an analysis of its performance.

A. Transmitted Signal

A block diagram of the proposed MPO-OFDM transmitter is shown in Fig. 1. To simplify the notation, we only analyze the signal in one OFDM symbol time and neglect the cyclic prefix required if operating in dispersive environments.

For MPO-OFDM, M-ary quadrature amplitude modulation (M-QAM) is applied for a high modulation efficiency in this paper. We assume that X_i is the M-QAM data modulated on the ith OFDM subcarrier. Without using Hermitian symmetry, the kth component after the inverse fast Fourier transform (IFFT) can be represented as

$$x[k] = \frac{1}{N}\sum_{i=0}^{N-1} X_i \exp\left(\frac{j2\pi ki}{N}\right). \quad (1)$$

where $X_i,\ \forall\ i$ are assumed to be independent and identically distributed random variable with $|X_i| \le 1$. After the parallel to serial converter, the mth time-domain sample of the OFDM symbol can be represented as $x_s[m] = \sum_{k=0}^{N-1} x[k]\delta[m-k]$, which is complex-valued. When N is large (usually 64 or greater), the real and imaginary parts of $x_s[m]$ can be modeled as independent Gaussian distributed variables with zero mean and variance σ_x^2 [12].

After the Cartesian to polar converter, the magnitude and phase information of $x_s[m]$ can be represented as $|x_s[m]|$ and $\angle x_s[m]$. The magnitude and phase components can be transmitted individually since they are real and non-negative valued. As shown in Fig. 1, a modulation index, β, is applied to control the scale of $|x_s[m]|$. Since large-valued signals beyond the power limit must be clipped, β can be controlled to trade off the clipping distortion and signal power. Therefore, we can optimally select β to maximize the SNR. The phase information, $\angle x_s[m]$, is quantized, encoded and transmitted using additional temporal frames by using

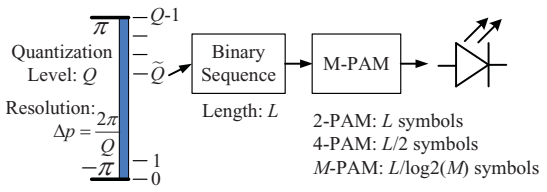

Fig. 2. Illustration of phase quantization with M-PAM coding.

M-PAM. The quantization level and modulation constellation size of M-PAM are two design parameters to be optimized in MPO-OFDM.

An illustration of quantizing and encoding the phase information for MPO-OFDM is shown in Fig. 2. In this figure, the phase information is quantized by Q levels using L bits, where $Q = 2^L$. Thus, the quantization resolution is denoted as $\Delta p = 2\pi/Q$. M-PAM is applied to transmit the phase information after quantization. The larger the modulation constellation size of the M-PAM, the fewer symbols are used to represent the phase. For an extreme case, using 2-PAM requires L binary symbols to present one phase information for each subcarrier. A smaller M-PAM modulation constellation size results in a larger number of symbols for the phase, which is more robust to the additive noise, yet requires a larger bandwidth when the data rate is fixed.

Fig. 3 illustrates examples of using different constellation size M-PAM to represent the phase. In this figure, frame 1 transmits the magnitude component, $|x_s[m]|,\ m = 0, 1, \cdots, N-1$, the value of which beyond the peak power, P_{max}, must be clipped. The other signal frames are used to transmit the phase information that is naturally constrained, thus no clipping distortion is introduced. Considering the bandwidth requirement and the noise effects on the phase, the modulation constellation size of the M-PAM used to transmit the phase can be optimally chosen.

B. Received Signal

At the receiver, if the channel loss is ignored, the received SNR for the M-PAM phase information can be approximated as $\gamma_p = P_{\max}^2/4N_0R_s$, where N_0 and R_s represent the noise spectral density and the transmitted OFDM symbol rate, respectively. Therefore, the bit error rate (BER) of the binary sequence demodulated from the M-PAM phase information

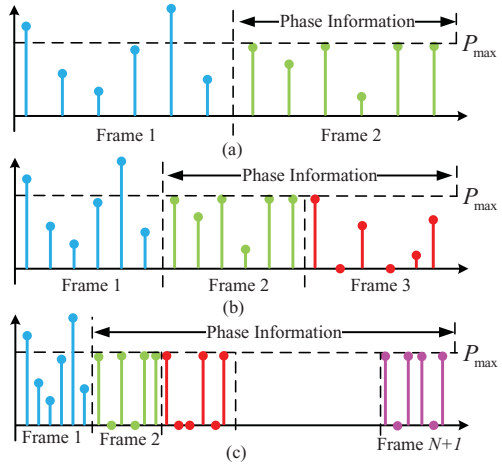

Fig. 3. Illustration of MPO-OFDM signals. (a) M-PAM with $M = Q$ is used to transmit the phase. (b) M-PAM with $M = Q/2$ is used to transmit the phase. (c) 2-PAM is used to transmit the phase.

can be approximately calculated by [13]

$$b_p \approx \frac{M_p - 1}{M_p \log_2 M_p} \mathrm{erfc}\left(\sqrt{\frac{\gamma_p}{(M_p-1)^2}}\right), \tag{2}$$

where $\mathrm{erfc}(\cdot)$ is the complementary error function, which is defined as $\mathrm{erfc}(x) = \frac{2}{\sqrt{\pi}} \int_x^\infty e^{-u^2} du$. After reconstructing the phase information, the equivalent additive noise variance can be approximated as

$$\begin{aligned} \sigma_p^2 \approx b_p \sum_{i=0}^{L-1} \left(2^i \Delta p\right)^2 + b_p^2 \sum_{i=0}^{L-2} \sum_{j=i+1}^{L-1} \left(2^i \Delta p + 2^j \Delta p\right)^2 \\ + b_p^3 \sum_{i=0}^{L-3} \sum_{j=i+1}^{L-2} \sum_{\ell=i+2}^{L-1} \left(2^i \Delta p + 2^j \Delta p + 2^\ell \Delta p\right)^2 + \cdots . \end{aligned} \tag{3}$$

As shown in Fig. 4, after sampling and using a polar to Cartesian converter, the nth sample for the received signal in one OFDM symbol can be represented as

$$\begin{aligned} r[n] = \left(\frac{\alpha\beta}{N} \sum_{i=0}^{N-1} X_i \exp\left(\frac{j2\pi}{N} ni\right) \right. \\ \left. + w_T[n] \right) \exp\left(j(\phi_p[n] + \phi_{\mathrm{qu}}[n])\right), \end{aligned} \tag{4}$$

where $\phi_p[n]$ and $\phi_{\mathrm{qu}}[n]$ represent equivalent additive and quantization noises added to the phase of the nth OFDM symbol. The variance of $\phi_p[n]$ and $\phi_{\mathrm{qu}}[n]$ are σ_p^2 and $\sigma_{\mathrm{qu}}^2 = (\Delta p)^2/12$, respectively. In (4), $w_T[n]$ represents the nth sample of the noise added to the magnitude component, which includes two parts, denoted as $w_T[n] = w_m[n] + w_c[n]$, where $w_m[n]$ and $w_c[n]$ represent the additive noise on the magnitude part and the clipping noise due to the peak power limit, respectively. $w_m[n]$ and $w_c[n]$ can be modeled as Gaussian distributed variables with zero means. The variance of $w_m[n]$ is $\sigma_m^2 = N_0 R_s$. The effects of the clipping are more complex,

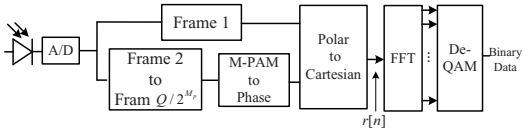

Fig. 4. Block diagram of the receiver in MPO-OFDM systems.

and we rely on a theorem referred to as the Bussgang theorem.

The Bussgang theorem allows us to characterize a clipped Gaussian signal as the sum of a Gaussian signal with a gain α and a Gaussian clipping noise with variance σ_c^2, after transmission through a non-linear system [14]. Based on this theorem, α describes the power loss due to the peak power clipping, which can be estimated by [14]

$$\begin{aligned} \alpha &= \frac{\mathrm{Var}(\varphi(\beta|x[k]|))}{\mathrm{Var}(\beta|x[k]|)} \\ &= 1 - \exp\left(\frac{-P_{\max}^2}{2\beta^2\sigma_x^2}\right)\left(\frac{P_{\max}^2}{2\beta^2\sigma_x^2} + 1\right) \end{aligned} \tag{5}$$

where the function $\mathrm{Var}(x)$ represents the variance of x [12]. $\varphi(x)$ models the nonlinear response of the transmitter, which is represented as

$$\varphi(x) = \begin{cases} P_{\max}, & x \geq P_{\max} \\ x, & P_{\max} > x > 0 \end{cases}. \tag{6}$$

The probability density function (pdf) of $\beta|x[k]|$ can be derived as

$$f(x,\beta) = \frac{x}{\beta^2\sigma_x^2} \exp\left(-\frac{x^2}{2\beta^2\sigma_x^2}\right), \tag{7}$$

where σ_x^2 represents the variance of $x[k]$, $\forall\ k$. Therefore, the variance of the clipping noise can be calculated as

$$\begin{aligned} \sigma_c^2 &= \int_{P_{\max}}^\infty (x - P_{\max})^2 f(x) dx \\ &= 2\beta^2\sigma_x^2 \exp\left(\frac{-P_{\max}^2}{2\beta^2\sigma_x^2}\right) - \sqrt{\pi} P_{\max} \mathrm{erfc}\left(\sqrt{\frac{P_{\max}^2}{2\beta^2\sigma_x^2}}\right). \end{aligned} \tag{8}$$

At the receiver, after the FFT, the M-QAM data of the qth subcarrier is represented as

$$\begin{aligned} y_q &= \sum_{n=0}^{N-1} r[n] \exp\left(-j\frac{2\pi}{N} nq\right) \\ &= \frac{\alpha\beta}{N} \sum_{i=0,}^{N-1} \sum_{n=0}^{N-1} X_i \exp\left(j\left(\frac{2\pi}{N} n(i-q) + \phi_p[n] + \phi_{\mathrm{qu}}[n]\right)\right) \\ &+ G_q \\ &= X_q \frac{\alpha\beta}{N} \sum_{n=0}^{N-1} \exp\left(j(\phi_p[n] + \phi_{\mathrm{qu}}[n])\right) \\ &+ \frac{\alpha\beta}{N} \sum_{\substack{i=0 \\ i\neq q}}^{N-1} \sum_{n=0}^{N-1} X_i \exp\left(j\left(\frac{2\pi}{N} n(i-q) + \phi_p[n] + \phi_{\mathrm{qu}}[n]\right)\right) \\ &+ G_q, \end{aligned} \tag{9}$$

where $G_q = \sum_{n=0}^{N-1} w_T[n] e^{-j\left(\frac{2\pi}{N} nq + \phi_p[n] + \phi_{\mathrm{qu}}[n]\right)}$, which is Gaussian distributed with zero mean. The variance of G_q, σ_G^2, is a function of σ_m^2, σ_c^2, σ_p^2, Δp and N, which can be calculated as

$$\sigma_G^2 = \frac{N\left(\sigma_m^2 + \sigma_c^2\right)\sin(\Delta p)}{\Delta p} \exp\left(-2\sigma_p^2\right). \tag{10}$$

Therefore, the SNR can be represented as

$$\gamma = \frac{\alpha^2\beta^2\sigma_x^2 E\{|\lambda(0)|^2\}}{\alpha^2\beta^2\sigma_x^2 \sum_{\ell=0}^{N-1} E\{|\lambda(\ell)|^2\} + \sigma_G^2}, \tag{11}$$

where $E\{\cdot\}$ denotes expectation, and $E\{|\lambda(\ell)|^2\}$ can be calculated as

$$\begin{aligned} &E\{|\lambda(\ell)|^2\} \\ &= \frac{1}{N^2} E\left\{\left|\sum_{n=0}^{N-1} \exp\left(j\left(\frac{2\pi}{N} n\ell + \phi_p[n] + \phi_{\mathrm{qu}}[n]\right)\right)\right|^2\right\} \\ &= \frac{\left(\mathrm{sinc}\left(\frac{\Delta p}{2}\right)\right)^2}{\exp(\sigma_p^2) N^2} \left\{\sum_{n=0}^{N-1} \sum_{\substack{m=0 \\ m\neq n}}^{N-1} \exp\left(j\left(\frac{2\pi}{N}(n-m)\ell\right)\right)\right\} \\ &\quad + \frac{1}{N}, \end{aligned} \tag{12}$$

where $\mathrm{sinc}(\cdot) = \sin(x)/x$. Using the expression of SNR in (11), the BER for the data can be approximated by using [13] as

$$\mathrm{BER} \approx \frac{\sqrt{M_d} - 1}{\sqrt{M_d}\log_2\left(\sqrt{M_d}\right)} \mathrm{erfc}\left(\sqrt{\frac{3\gamma}{2(M_d - 1)}}\right), \tag{13}$$

where M_d represents the modulation constellation size for the QAM data.

III. Numerical Results

Numerical results of the performance of the proposed MPO-OFDM are shown in this section. MPO-OFDM is compared with ACO-, DCO-, U- and polar-based OFDM as benchmarks. To make the comparison fair, the OFDM symbol rate for techniques that use the same modulation is the same. The results shown are derived from the analysis shown above; they have been validated through simulation. Unless otherwise noted, the parameters used to obtain the numerical results are shown in Table I. In addition, the system bandwidth constraint is not taken into account in this paper.

TABLE I
Parameters Used for Numerical Results

Channel loss	1
Responsivity	0.5 A/W
Peak optical power limit, $P_{\max}$	10 mW
Number of subcarriers, N	64
Phase quantization levels, Q	64
Noise spectral density, N_0	3×10^{-11} mW/Hz
OFDM symbol rate	140 Mbps

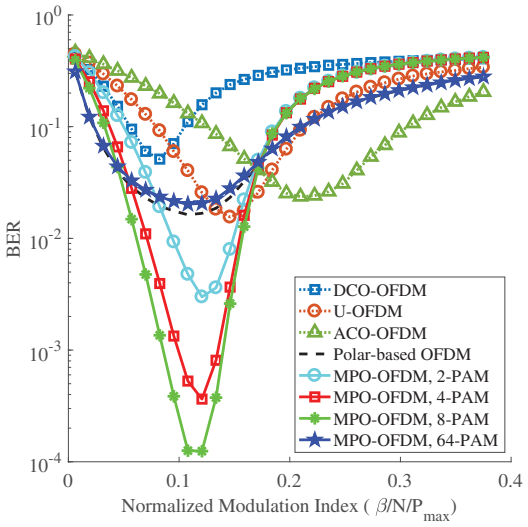

Fig. 5. BER comparison of DCO-, ACO-, U-, MPO- and polar-based OFDM using 64-level quantization for the phase. 64-QAM is applied for all techniques.

An adjustable modulation index, β, controlling the OFDM signal scale, is applied in all the OFDM techniques tested in this paper. Considering the peak radiation power constraint, the modulation index can be optimally chosen to trade off the clipping distortion and signal power. In Fig. 5, the BER performance for all the techniques can be seen to first improve as the modulation index increases. Then, further increasing the modulation index introduces severe clipping distortion on the magnitude of the OFDM signal that impacts the BER performances. Comparing the proposed MPO-OFDM with DCO-, ACO- and U-OFDM, MPO-OFDM can achieve a better BER performance when choosing the proper parameters. Since MPO-OFDM does not require Hermitian symmetry to generate real-valued signals, it has a better bandwidth utilization efficiency than ACO- and U-OFDM. In addition, the phase information component of the MPO-OFDM signal does not experience peak power clipping, which results in less nonlinear distortion than DCO-OFDM.

For MPO-OFDM, the M-PAM constellation size chosen for transmitting the phase information affects the system performance. The smaller the modulation constellation size for M-PAM, the less the additive noise affects the signal. However, the smaller the modulation constellation size, the more symbols we need to send to represent one OFDM symbol, which requires a wider bandwidth, resulting in more noise for a fixed noise spectral density. Therefore, the modulation constellation size for M-PAM can be optimally selected to provide the better performance for a given phase quantization level. In Fig. 5, 2-, 4-, 8- and 64-PAM are tested to encode the quantized phase signal, and 8-PAM is shown to provide the best BER performance for the system parameters tested. The proposed MPO-OFDM suffers less from the noise added to the phase information and outperforms polar-based

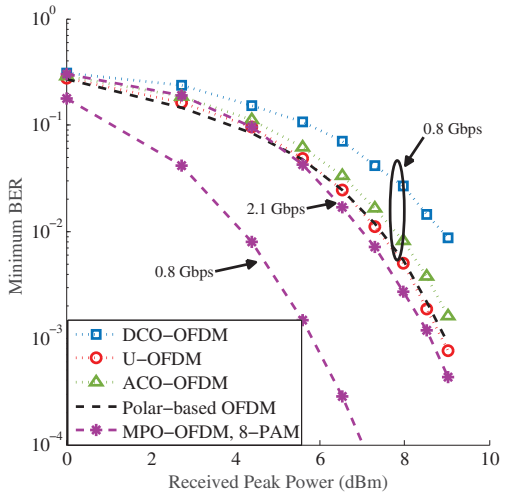

Fig. 6. BER comparison of DCO-, ACO-, U-, MPO- and polar-based OFDM using different received peak power.

OFDM when 2-, 4-, and 8-PAM are used. Using 64-PAM, MPO-OFDM uses the same number of frames to transmit the magnitude and phase information as polar-based OFDM does. Therefore, MPO-OFDM with 64-PAM performs slightly worse than polar-based OFDM due to the quantization noise.

Fig. 6 shows a BER comparison for different received peak optical powers. In this figure, the optimal β is used for each technique to achieve the minimum BER for each power level. In general, the proposed MPO-OFDM can provide a better BER performance than other techniques tested. For the same bit rate, MPO-OFDM with 8-PAM coded phase information has more than a 2 dB power advantage over polar-based OFDM using the same parameters in Table I. Comparing MPO- and polar-based OFDM with a similar BER performance, the proposed MPO-OFDM can achieve more than twice the bit rate than polar-based OFDM due to its ability to reduce the effects of additive noise.

IV. Conclusion

In this paper, we propose a new OFDM scheme for IM/DD systems we call the magnitude-phase OFDM. Similar to polar-based OFDM, the proposed MPO-OFDM does not require Hermitian symmetric QAM data to generate a real transmitted signal. Instead, the magnitude and phase information of the complex-valued OFDM signal are transmitted, successively. Unlike polar-based OFDM, the proposed MPO-OFDM encodes the quantized phase information to reduce the interference introduced by the additive noise on the phase. M-PAM is used to transmit the encoded and quantized phase information. Due to the peak radiation power constrained transmitters, the magnitude information experiences nonlinear distortion caused by the peak power clipping. Therefore, by trading off the clipping distortion and signal power, we can optimally select the modulation index to obtain the highest SNR. For the same bit rate, the proposed MPO-OFDM can provide a better minimum BER performance than DCO-, ACO-, U- and polar-based OFDM when proper design parameters are chosen. Alternatively, the proposed MPO-OFDM can achieve more than twice the data rate than the OFDM techniques tested with a similar BER performance.

In future work, a bandlimited light source and dispersive channel will be considered. For visible light communication systems, dimming control and the effects of different illumination requirements on MPO-OFDM will be explored.

Acknowledgement

This work was funded in part by the National Science Foundation (NSF) through the STTR program, under award number 1521387, and VLNComm, Inc.

References

[1] A. Jovicic, J. Li, and T. Richardson, "Visible light communication: opportunities, challenges and the path to market," *IEEE Commun. Mag.*, vol. 51, no. 12, pp. 26–32, December 2013.

[2] T. Komine and M. Nakagawa, "Fundamental analysis for visible-light communication system using LED lights," *IEEE Trans. Consum. Electron.*, vol. 50, no. 1, pp. 100–107, Feb 2004.

[3] A. Azhar, T. Tran, and D. O'Brien, "A Gigabit/s indoor wireless transmission using MIMO-OFDM visible-light communications," *IEEE, Photon. Technol. Lett.*, vol. 25, no. 2, pp. 171–174, 2013.

[4] H. Elgala, R. Mesleh, and H. Haas, "Indoor optical wireless communication: potential and state-of-the-art," *IEEE Commun. Mag.*, vol. 49, no. 9, pp. 56–62, 2011.

[5] C. Chen, D. Tsonev, and H. Haas, "Joint transmission in indoor visible light communication downlink cellular network," in *2013 IEEE Global Commun. Conf. (GLOBECOM)*, 2013, pp. 1127–1132.

[6] M. Zhang and Z. Zhang, "An optimum DC-biasing for DCO-OFDM system," *IEEE Commun. Lett.*, vol. 18, no. 8, pp. 1351–1354, Aug 2014.

[7] J. Armstrong and A. J. Lowery, "Power efficient optical OFDM," *Elect. Lett.*, vol. 42, no. 6, pp. 370–372, March 2006.

[8] S. D. Dissanayake and J. Armstrong, "Comparison of ACO-OFDM, DCO-OFDM and ADO-OFDM in IM/DD systems," *J. Lightw. Technol.*, vol. 31, no. 7, pp. 1063–1072, April 2013.

[9] T. Q. Wang and X. Huang, "Fractional reverse polarity optical OFDM for high speed dimmable visible light communications," *IEEE Trans. on Commun.*, vol. 66, no. 4, pp. 1565–1578, 2018.

[10] D. Tsonev, S. Sinanovic, and H. Haas, "Novel unipolar orthogonal frequency division multiplexing (U-OFDM) for optical wireless," in *2012 IEEE 75th Veh. Technol. Conf. (VTC Spring)*, May 2012, pp. 1–5.

[11] H. Elgala and T. D. C. Little, "Polar-based OFDM and SC-FDE links toward energy-efficient Gbps transmission under IM-DD optical system constraints," *IEEE/OSA Journal of Optical Communications and Networking*, vol. 7, no. 2, pp. A277–A284, February 2015.

[12] J. Armstrong, "OFDM for optical communications," *J. Lightw. Technol.*, vol. 27, no. 3, pp. 189–204, Feb 2009.

[13] Z. Ghassemlooy, W. Popoola, and Rajbhandari, *Optical Wireless Communications: System and Channel Modeling with Matlab*. CRC Press, 2013.

[14] R. Price, "A useful theorem for nonlinear devices having gaussian inputs," *IRE Transactions on Information Theory*, vol. 4, no. 2, pp. 69–72, June 1958.